

Article

Near-Horizon Thermodynamics of Hairy Black Holes from Gravitational Decoupling

Rogério Teixeira Cavalcanti ^{1,2}, Kelvin dos Santos Alves ² and Julio Marny Hoff da Silva ^{2,*}

¹ Centro de Matemática, Computação e Cognição, Universidade Federal do ABC, Santo André 09210-580, Brazil; rogerio.cavalcanti@ufabc.edu.br

² Departamento de Física, Universidade Estadual Paulista (Unesp), Guaratinguetá 12516-410, Brazil; kelvin.santos@unesp.br

* Correspondence: julio.hoff@unesp.br

Abstract: The horizon structure and thermodynamics of hairy spherically symmetric black holes generated by the gravitational decoupling method are carefully investigated. The temperature and heat capacity of the black hole is determined, as well as how the hairy parameters affect the thermodynamics. This allows for an analysis of thermal stability and the possible existence of a remanent black hole. We also calculate the Hawking radiation corrected by the generalized uncertainty principle. We consider the emission of fermions and apply the tunneling method to the generalized Dirac equation. This shows that, despite the horizon location being the same as the Schwarzschild one for a suitable choice of parameters, the physical phenomena that occur near the horizon of both black holes are qualitatively different.

Keywords: gravitational decoupling; hairy black holes; black hole thermodynamics; Hawking radiation; remanent black hole; generalized uncertainty principle; tunnelling method

PACS: 04.70.-s; 04.70.Dy; 03.65.Xp



Citation: Cavalcanti, R.T.; Alves, K.d.S.; Hoff da Silva, J.M.

Near-Horizon Thermodynamics of Hairy Black Holes from Gravitational Decoupling. *Universe* **2022**, *8*, 363. <https://doi.org/10.3390/universe8070363>

Academic Editor: Carlos Herdeiro

Received: 19 May 2022

Accepted: 27 June 2022

Published: 1 July 2022

Publisher's Note: MDPI stays neutral with regard to jurisdictional claims in published maps and institutional affiliations.



Copyright: © 2022 by the authors. Licensee MDPI, Basel, Switzerland. This article is an open access article distributed under the terms and conditions of the Creative Commons Attribution (CC BY) license (<https://creativecommons.org/licenses/by/4.0/>).

1. Introduction

Black hole physics plays a central role in contemporary high-energy physics research [1], from scales ranging from cosmology to astrophysics [2] to elementary particle physics [3]. The emergence of observational proposals for investigating these objects was made possible after the seminal results of Penrose, Hawking, Geroch, Israel, Carter and others, which put geometry and physics of black hole solutions over a solid basis. Among the central results, could be pinpointed: the classic definition of the event horizon, the singularity theorems by Penrose, Hawking and Geroch, the no-hair theorem, the cosmic censorship hypothesis, and the formation of trapped surfaces under generic conditions during gravitational collapse. Notably, strong observational evidence in astrophysics has been accumulating since the 1970s [2], including evidence that culminated in the nobel prize for Reinhard Genzel [4] and Andrea M. Ghez [5], the LIGO detections of gravitational waves [6] and the image captured by the Event Horizon Telescope collaboration [7]. Black holes are closely linked to some of the most powerful processes known in physics, such as the gravitational collapse of stars, active galactic nuclei, and the aforementioned gravitational waves emitted by binary black hole systems. Formally, black holes are characterized by the existence of horizons bounding two causally disconnected regions [8,9]. Their most important feature is, then, not the existence of singularity, which has no support in a well-defined gravitational theory, but instead the existence of an event horizon covering its interior. While the characterization of stationary and asymptotically flat hole horizons in general relativity is well-known [10], the physical understanding of the horizon nature of solutions beyond general relativity (or even non-stationary ones) have generated extensive research in recent years [9,11–13]. In the development of black hole mechanics and thermodynamics, which culminated

in Bekenstein's second law of generalized thermodynamics and Hawking radiation, the horizon also occupies a central role. However, the definition of event horizon inspired by stationary black holes turns out to be of little use in investigations into objects with less symmetric dynamics. This major obstacle manifests in the fact that the precise event horizon definition would require knowledge of the entire spacetime history, which is obviously not physically achievable [11].

On the other hand, there are alternative gravitation theories to general relativity. This may include the existence of non-minimally curvature-coupled scalar fields or terms with higher order derivatives in the action, which has direct consequences for the uniqueness theorems of black hole type solutions in general relativity. In fact, the famous no hair theorem is not preserved outside the domain of general relativity. These solutions could lead to detectable effects in the astrophysical black hole horizon vicinity [14,15]. Finding physically relevant solutions to the Einstein field equations is not an easy task. However, deriving new solutions from other, previously known solutions is a widespread technique in general relativity. Recently, the so-called gravitational decoupling (GD) method has attracted the attention of the community due to its simplicity and effectiveness [16–18]. This allows for one to generate new, exact analytical solutions to Einstein's equations by considering additional sources to the stress-energy tensor, including the description of anisotropic stellar distributions [19,20], whose predictions might be tested in astrophysical observations [21–24]. The recent discovery of hairy black hole solutions by gravitational decoupling is particularly interesting. These solutions describe a black hole with hair represented by generic fields surrounding the central source of the vacuum Schwarzschild metric, requiring the existence of a well-defined event horizon and hair that obeys the strong energy conditions outside the horizon [18]. Some interesting consequences of these hairy black holes have been investigated [25–27], and there is much to be done in the future.

Finally, it is usually believed that a minimal length in the spacetime is related to a generalization of the uncertainty principle in a plethora of theories and models [28–34]. The link between these may be heuristically described [35] by noticing that, in natural units, the Schwarzschild radius, r_s , scales as $r_s \sim M$. In higher energies, where small-length scales are indeed scrutinized, the previous relation reads $\Delta x \sim \Delta p$, so that the typical product $\Delta x \Delta p$ has a correction proportional to Δp^2 . Since black holes are *per se* physical systems under extreme conditions, their neighborhood is the natural place to investigate quantum effects in the scope of the generalized uncertainty principle.

This paper is organized as follows: Section 2 is dedicated to introducing basic facts about the horizon structure of the hairy black hole obtained by the gravitational decoupling procedure, obtaining three different metrics for gravitational decoupled hairy black holes. This includes an analysis of the role of the ℓ and α parameters in the resulting horizon structure. In Section 3, we investigate quantum near-horizon effects of the hairy black hole, namely the correction of the Hawking radiation coming from the Dirac equation considering the generalized uncertainty principle. Section 4 is dedicated to the conclusions.

2. Hairy Horizons and Gravitational Decoupling

The extended gravitational decoupling method (EGD), introduced in [16], is a powerful technique for simplifying the Einstein's field equations when additional fonts are considered in a previously known seed spacetime. Departing from the Einstein's field equations,

$$G_{\mu\nu} = 8\pi \check{T}_{\mu\nu}, \quad (1)$$

where $G_{\mu\nu} = R_{\mu\nu} - \frac{1}{2}Rg_{\mu\nu}$ denotes the Einstein tensor; the method assumes that the energy-momentum tensor can be split as

$$\check{T}_{\mu\nu} = T_{\mu\nu} + \Theta_{\mu\nu}. \quad (2)$$

The $T_{\mu\nu}$ regards a perfect fluid that is source of a known solution of general relativity, whereas $\Theta_{\mu\nu}$ may contain new fields or an extension of the gravitational sector.

The conservation equation $\nabla_\mu \check{T}^{\mu\nu} = 0$ must also hold. By inspecting the field equations it is possible to identify the effective density, tangential and radial pressures

$$\check{\rho} = \rho + \Theta_0^0, \tag{3a}$$

$$\check{p}_t = p - \Theta_2^2, \tag{3b}$$

$$\check{p}_r = p - \Theta_1^1. \tag{3c}$$

The idea is take a spherically symmetric solution to the field equations and deform it in such a way that the field equations split in a sector containing the known solution and another one for the deformation. Indeed, assuming a known spherically symmetric metric

$$ds^2 = -e^{\kappa(r)} dt^2 + e^{\zeta(r)} dr^2 + r^2 d\Omega^2, \tag{4}$$

and deforming $\kappa(r)$ and $\zeta(r)$ as

$$\kappa(r) \mapsto \kappa(r) + \alpha f_2(r) \tag{5a}$$

$$e^{-\zeta(r)} \mapsto e^{-\zeta(r)} + \alpha f_1(r), \tag{5b}$$

the resulting field equations split into two distinct arrays. The first one is for the source $T_{\mu\nu}$, whose solution is given by the metric (4). The second encompasses $\Theta_{\mu\nu}$, as well as the deformation functions $f_1(r)$ and $f_2(r)$, to be determined by the field equations. This reads

$$8\pi \Theta_0^0 = \alpha \left(\frac{f_1}{r^2} + \frac{f_1'}{r} \right), \tag{6a}$$

$$8\pi \Theta_1^1 - \alpha \frac{e^{-\zeta} f_2'}{r} = \alpha f_1 \left(\frac{1}{r^2} + \frac{\kappa'(r) + \alpha f_2'(r)}{r} \right) \tag{6b}$$

$$8\pi \Theta_2^2 - \alpha f_1 Z_1(r) = \alpha \frac{f_1'}{4} \left(\kappa'(r) + \alpha f_2'(r) + \frac{2}{r} \right) + \alpha Z_2(r) \tag{6c}$$

where [16]

$$Z_1(r) = \alpha^2 f_2'(r)^2 + 2\alpha \left(f_2'(r)\kappa'(r) + \frac{f_2''(r)}{r} + f_2''(r) \right) + \kappa'(r)^2 + \frac{2\kappa'(r)}{r} + 2\kappa''(r) \tag{7a}$$

$$Z_2(r) = \alpha e^{-\zeta} \left(2f_2'' + f_2^{2'} + \frac{2f_2'}{r} + 2\kappa' f_2' - \zeta' f_2' \right). \tag{7b}$$

The above equations show that $\Theta_{\mu\nu}$ must vanish when the deformations parameter α vanishes. It finishes the main setup of the gravitational decoupling procedure. To find a black hole solution with a well-defined horizon structure, in Reference [18] the Schwarzschild solution was assumed in place of Equation (4), demanding that $g_{rr} = -\frac{1}{g_H}$ for the deformed metric, namely

$$\left(1 - \frac{2M}{r} \right) \left(e^{\alpha f_2(r)} - 1 \right) = \alpha f_1(r). \tag{8}$$

Therefore,

$$ds^2 = - \left(1 - \frac{2M}{r} \right) e^{\alpha f_2(r)} dt^2 + \left(1 - \frac{2M}{r} \right)^{-1} e^{-\alpha f_2(r)} dr^2 + r^2 d\Omega^2. \tag{9}$$

Further, assuming strong energy conditions,

$$\check{\rho} + \check{p}_r + 2\check{p}_t \geq 0, \tag{10a}$$

$$\check{\rho} + \check{p}_r \geq 0, \tag{10b}$$

$$\check{\rho} + \check{p}_t \geq 0, \tag{10c}$$

and managing the field equations, a new hairy black hole solution was found [18]

$$ds^2 = -f(r)dt^2 + \frac{1}{f(r)}dr^2 + r^2d\Omega^2, \tag{11}$$

where

$$f(r) = 1 - \frac{2M + \alpha\ell}{r} + \alpha e^{-\frac{r}{M}}. \tag{12}$$

The dimensionless parameter α keeps track of the deformation of the Schwarzschild black hole and ℓ , whose dimensions and length are a constant, appearing as a result of a non-vanishing additional form $\Theta_{\mu\nu}$. Notice that, by taking $\alpha = 0$, we recover the Schwarzschild solution. As a result of the strong energy condition, the ℓ parameter is restricted to $\ell \geq 2M/e^2$, whose extremal case $\ell = 2M/e^2$ results

$$f(r) = 1 - \frac{2M}{r} + \alpha \left(e^{-\frac{r}{M}} - \frac{2M}{e^2 r} \right). \tag{13}$$

The hairy black hole has only one horizon, located at $r = r_H$, such that

$$r_H - 2M - \alpha\ell + r_H\alpha e^{-\frac{r_H}{M}} = 0. \tag{14}$$

Such an equation has no analytical solution, except for specific values of the parameters (α, ℓ) . In particular, for the extreme case, the horizon is located at $r_H = 2M$. The Equation (14), however, can be analyzed numerically. Figure 1 shows the horizon radius for different values of the parameters (α, ℓ) in the range allowed by the strong-energy condition.

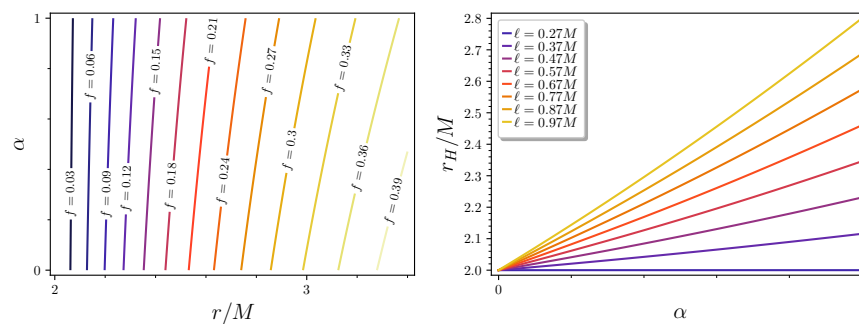


Figure 1. Left panel: Contour lines of $f(r)$ depending on (r, α) for the extreme case ($\ell = 2Me^{-2}$). Right panel: Radius of the hairy black hole horizon r_H as function of α for different values of the parameter ℓ . The non-linearity of Equation (14) has little influence on r_H .

To investigate the horizon structure of the above hairy black hole, we are going to perform a coordinate transformation to an analogous to the advanced Eddington–Finkelstein coordinates, so that $(t, r, \theta, \phi) \mapsto (v, r, \theta, \phi)$ and v is given by

$$v = t - \int \left(1 - \frac{2M + \alpha\ell}{r} + \alpha e^{-\frac{r}{M}} \right)^{-1} dr. \tag{15}$$

In those new coordinates, the metric (11) takes the form

$$ds^2 = - \left(1 - \frac{\alpha\ell + 2M}{r} + \alpha e^{-\frac{r}{M}} \right) dv^2 + 2dvdr + r^2d\Omega^2, \tag{16}$$

with the advantage of being regular on the horizon. In fact, the only physical singularity is at $r = 0$ [18], as can be seen from the Kretschmann scalar,

$$K = \frac{48 M^2}{r^6} - 8 \alpha \left(\frac{2 M e^{-\frac{r}{M}}}{r^5} + \frac{2 e^{-\frac{r}{M}}}{r^4} + \frac{e^{-\frac{r}{M}}}{M r^3} - \frac{6 M \ell}{r^6} \right) - \alpha^2 \left(\frac{8 \ell e^{-\frac{r}{M}}}{r^5} + \frac{8 \ell e^{-\frac{r}{M}}}{M r^4} + \frac{4 \ell e^{-\frac{r}{M}}}{M^2 r^3} - \frac{e^{-\frac{2r}{M}}}{M^4} - \frac{4 e^{-\frac{2r}{M}}}{r^4} - \frac{4 e^{-\frac{2r}{M}}}{M^2 r^2} - \frac{12 \ell^2}{r^6} \right). \tag{17}$$

We also need the normal null vectors l and k , so that $l_\mu l^\mu = k_\mu k^\mu = 0, l_\mu k^\mu = -1$. These vectors are explicitly given by

$$l = \partial_v + \frac{1}{2} \left(1 - \frac{2M + \alpha \ell}{r} + \alpha e^{-\frac{r}{M}} \right) \partial_r, \tag{18}$$

$$k = -\partial_r. \tag{19}$$

As can be seen, they are linearly independent, future-pointing and associated with the null geodesics outgoing and ingoing the horizon, respectively. This allows for us to introduce metric on the horizon cross-section [12]

$$q_{\mu\nu} = g_{\mu\nu} + l_\mu k_\nu + k_\mu l_\nu \longrightarrow q = r^2 d\theta^2 + r^2 \sin^2 \theta d\phi^2, \tag{20}$$

as well as the expansion along the null normals

$$\theta_{(l)} = \frac{1}{2} \mathcal{L}_l \det(q) = \frac{1}{r} \left(1 - \frac{2M + \alpha \ell}{r} + \alpha e^{-\frac{r}{M}} \right), \tag{21}$$

$$\theta_{(k)} = \frac{1}{2} \mathcal{L}_k \det(q) = -\frac{2}{r}, \tag{22}$$

where \mathcal{L}_l denotes the Lie derivative along l . As expected, on the horizon

$$\theta_{(l)} \Big|_{r=r_H} = 0, \tag{23}$$

$$\theta_{(k)} \Big|_{r=r_H} = -\frac{2}{r_H} < 0. \tag{24}$$

These results show that the cross-section is a marginally trapped surface [12] and that the hairy horizon is a non-expanding horizon [36] (see Figure 2).

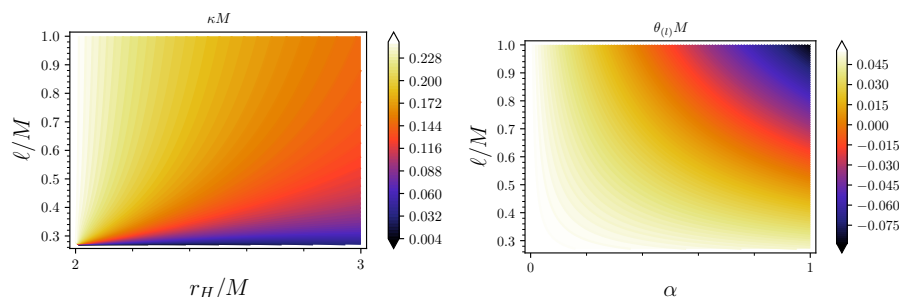


Figure 2. Left panel: gravitational constant κ (color scale) as function of the horizon radius r_H and hairy parameter ℓ . The decoupling parameters α were eliminated using Equation (14). The Schwarzschild case corresponds to the extreme left vertical line. Right panel: expansion of the cross-section (color scale) along the null vector l for $r = 2.3$. Notice that, close to the upper right corner, $r_H > 2.3$ (see Figure 1), resulting in a negative expansion.

Furthermore, since, on the horizon, the null normal l coincides with the killing vector $\zeta = \partial_v$, it is also a Killing horizon, whose associated gravitational surface is given by

$$\kappa = \left[\nabla_\mu l^\mu - \theta_{(l)} \right]_{r=r_H} = \frac{M}{r_H^2} + \frac{\alpha}{2} \left(\frac{\ell}{r_H^2} - \frac{e^{-\frac{r_H}{M}}}{M} \right). \tag{25}$$

This straightforwardly gives the Hawking temperature of the hairy black hole,

$$T_H = \frac{\kappa}{2\pi} = \frac{1}{2\pi} \left[\frac{M}{r_H^2} + \frac{\alpha}{2} \left(\frac{\ell}{r_H^2} - \frac{e^{-\frac{r_H}{M}}}{M} \right) \right]. \tag{26}$$

Eliminating the decoupling parameters α by means of Equation (14) we find

$$T_H = \frac{\left(\ell e^{\frac{r_H}{M}} - 2M + 2r_H \right) M - r_H^2}{2 \left(\ell e^{\frac{r_H}{M}} - r_H \right) M r_H}. \tag{27}$$

For the extreme case, this simplifies to

$$T_H = \frac{1}{8\pi M} \left(1 - \frac{\alpha}{e^2} \right) = T_{\text{Shw}} \left(1 - \frac{\alpha}{e^2} \right), \tag{28}$$

where $T_{\text{Shw}} = \frac{1}{8\pi M}$ is the Hawking temperature of the Schwarzschild black hole. Notice that, when compared to the Schwarzschild case, the extreme hairy black hole is slightly colder. Furthermore, for ℓ close to the extreme value $2Me^{-2}$, the Hawking temperature $T_H \rightarrow 0$ (see Figure 3). In the next section, we extend this result to a generalized uncertainty principle (GUP) scenario and fermionic emission, such as Hawking radiation.

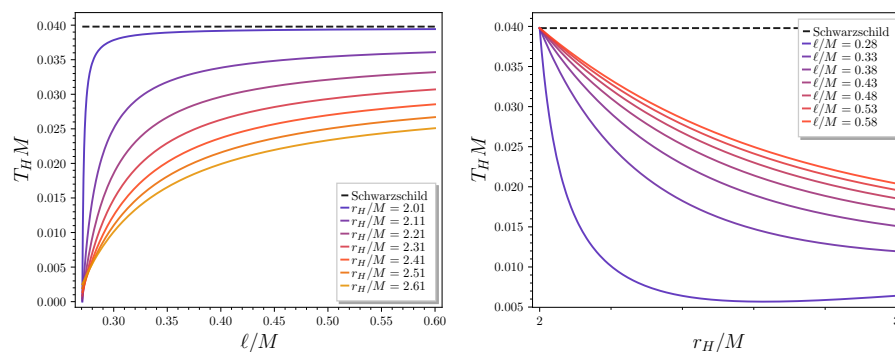


Figure 3. Left panel: Hawking temperature of hairy black holes depending on hairy parameter ℓ for different values of the horizon radius r_H . Notice the low temperature for $\ell \rightarrow 2Me^{-2}$. Right panel: Hawking temperature of hairy black holes depending on horizon radius r_H for different values of the hairy parameter ℓ . When $r_H \rightarrow 2M$, the temperature $T_H \rightarrow T_{\text{Shw}}$ for any ℓ . In both cases, the decoupling parameter α was eliminated using Equation (14) and the radius $r_H = 2M$ corresponds to the extreme case.

Since the field equations come from the standard Einstein–Hilbert action, the entropy of the hairy black hole shall be the Bekenstein–Hawking entropy,

$$S = \pi r_H^2. \tag{29}$$

In order to examine the thermal stability of the hairy black hole, we should find the heat capacity at constant ℓ , given by

$$C_\ell = T \left(\frac{\partial S}{\partial T} \right)_\ell = T \left(\frac{\partial S}{\partial r_H} \right)_\ell \left(\frac{\partial T}{\partial r_H} \right)_\ell^{-1} \tag{30}$$

$$= - \frac{2\pi (r_H^2 - \ell e^{r_H} - 2r_H + 2)r_H^2}{r_H^3 - 2r_H^2 - 2\ell e^{r_H} + 4}. \tag{31}$$

The discontinuity of the heat capacity, as shown in Figure 4, reflects the appearance of a Hawking–Page-like phase transition [37], separating regions of stable and unstable

domains. Such discontinuities appear only for small ℓ and relatively small r_H , namely, for $\ell \lesssim 0.35$ and $r_H \lesssim 5$, beyond which the heat capacity tends to saturate. The heat capacity is also well-behaved when $r_H = 2M$, regardless of ℓ . Again, this highlights that the exotic behaviour of the hairy black hole is only manifested for small r_H and small ℓ , but beyond $r_H = 2M$ and the extreme case ($\ell = 2Me^{-2}$). Furthermore, from the heat capacity plots in Figure 4, left panel, we see that when increasing ℓ , the discontinuity points become closer and closer, eventually merging and consequently turning the discontinuity into a peak. This, in turn, spreads to saturation.

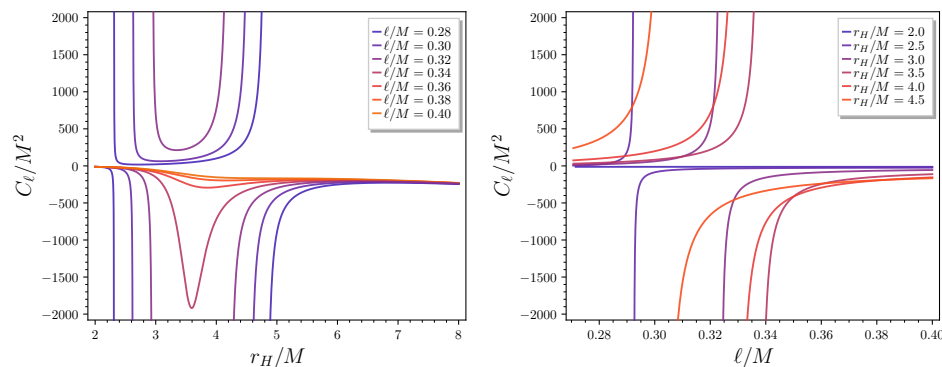


Figure 4. Left panel: heat capacity of hairy black holes depending on the horizon radius r_H for different values of hairy parameter ℓ . Right panel: heat capacity of hairy black holes depending on the hairy parameter ℓ for different values of the horizon radius r_H . In both cases the decoupling parameter α was eliminated using Equation (14) and the radius $r_H = 2M$ corresponds to the extreme case. Notice the discontinuities for $\ell < 0.36$ and $r_H < 5$.

3. Quantum Effects Near the Horizon

3.1. GUP and Generalized Dirac Equation

Minimum lengths are predicted from different approaches to quantum gravity, such as string theory [28,29], loop quantum gravity [30], quantum black holes [31], among others [32–34]. Some of those efforts have led to the so-called Generalized Uncertainty Principle (GUP), from where the minimum length naturally rises,

$$\Delta x \Delta p \geq \frac{\hbar}{2} [1 + \beta \Delta p^2], \tag{32}$$

where $\beta = \beta_0/m_p^2$, m_p is the Planck mass and β_0 is a dimensionless parameter. In order to encompass the effects coming from the GUP, in Ref. [38] modifications were made to the commutation relations $[x_i, p_j] = i\hbar\delta_{ij} [1 + \beta p^2]$, where x_i and p_i are position and momentum operators defined by $x_i = x_{0i}$ and $p_i = p_{0i}(1 + \beta p^2)$ respectively, where x_{0i} and p_{0j} satisfy the standard commutation relations. Therefore, keeping only the first order in β , one has

$$p^2 \simeq -\hbar^2 [\partial_i \partial^i - 2\beta \hbar^2 (\partial^i \partial_j) (\partial^j \partial_i)]. \tag{33}$$

According to [39], quantum gravity effects engender (as a net effect) a generalized frequency, with $E = i\hbar\partial_0$, given by $\tilde{\omega} = E(1 - \beta E^2)$. Now, by considering the energy mass shell condition $p^2 + m^2 = E^2$, the expression of energy in this context reads [39–42]

$$\tilde{E} = E[1 - \beta(p^2 + m^2)]. \tag{34}$$

In what follows, we investigate the radiation of spin-1/2 fermions in curved spacetime where the effects of quantum gravity are taken into account. This is carried out by means of the curved spacetime version of the generalized Dirac equation [41]. The usual curved spacetimes version is given by

$$(i\hbar\gamma^a e^{\mu}_a D_{\mu} + m) \Psi_{\uparrow}(t, r, \theta, \phi) = 0, \tag{35}$$

where

$$D_\mu = \partial_\mu + \frac{i}{2} \omega_\mu^{ab} \Sigma_{ab} \equiv \partial_\mu + \Omega_\mu, \tag{36}$$

with $\Sigma^{ab} = \frac{i}{4} [\gamma^a, \gamma^b]$; γ^d are the Clifford algebra generators for the Minkowski spacetime, ω_μ^{ab} are the spin connection coefficients and e^μ_a are the vierbein fields

$$g^{\mu\nu} = e^\mu_a e^\nu_b \eta^{ab}. \tag{37}$$

We adopt the convention that lowercase latin indexes denote the vierbein flat spacetime index, whereas Greek indexes are the curved spacetime ones. To avoid confusion, we label them as the spacetime coordinates (t, r, θ, ϕ) for curved spacetime and numbers for the flat one.

Combining Equations (33)–(35), and neglecting higher orders of β , the generalized Dirac equation in curved spacetime is found [41,43]

$$-i\hbar\gamma^0\partial_0\Psi_\uparrow(t, r, \theta, \phi) = \left(i\hbar\gamma^i\partial_i + i\hbar\gamma^\mu\Omega_\mu + m \right) \left(1 + \beta\hbar^2\partial_j\partial^j - \beta m^2 \right) \Psi_\uparrow(t, r, \theta, \phi). \tag{38}$$

This equation shall be used to derive corrections to the Hawking temperature by considering the GUP.

3.2. Corrected Fermionic Tunneling through Hairy Horizon

In this section, we are interested in corrected spin-1/2 fermions emission as Hawking radiation. This type of emission is expected due to the fact that black holes are surrounded by a thermal bath of finite temperature, from which point all sorts of particles could emerge [44,45]. The key point here is replacing Dirac’s equation by its generalized version, as introduced in the previous section. As we are going to see, this produces new corrections to the Hawking radiation of hairy black holes. Apart from replacing Dirac’s equation, the procedure is the usual one for the tunneling method [45–48]. The first point consists of choosing a spin-up or spin-down spinor and applying the WKB approximation. For the spin up, for example, we have:

$$\Psi_\uparrow(t, r, \theta, \phi) = \begin{pmatrix} A(t, r, \theta, \phi) \\ 0 \\ B(t, r, \theta, \phi) \\ 0 \end{pmatrix} \exp \left[\frac{i}{\hbar} I_\uparrow(t, r, \theta, \phi) \right], \tag{39}$$

where $A(t, r, \theta, \phi), B(t, r, \theta, \phi)$ are complex functions of the spacetime coordinates. One can, therefore, substitute the above spinor back into Dirac’s equation and find the imaginary part of the action. In fact, the imaginary radial part encodes the tunnelling probability which, by setting it, equals the Boltzmann factor and gives the temperature. Before proceeding, note that, by applying the operator $\hbar D_\mu$ to Ψ_\uparrow , most of the resulting terms are higher-order in \hbar . In fact,

$$\hbar D_\mu \Psi_\uparrow(t, r, \theta, \phi) = \hbar \begin{pmatrix} \partial_\mu A \\ 0 \\ \partial_\mu B \\ 0 \end{pmatrix} e^{\frac{i}{\hbar} I_\uparrow} + i\partial_\mu I_\uparrow \Psi_\uparrow - \frac{\hbar}{8} \omega_\mu^{ab} \Sigma_{ab} \Psi_\uparrow \tag{40}$$

$$= i\partial_\mu I_\uparrow \Psi_\uparrow + \mathcal{O}(\hbar). \tag{41}$$

Accordingly, we have to consider only the action derivative term for the usual Dirac operator. Here, we are going to use the extreme case of the hairy black hole metric, given by

$$ds^2 = -f(r)dt^2 + \frac{1}{f(r)}dr^2 + r^2d\Omega^2, \tag{42}$$

with $f(r) = 1 - \frac{2M}{r} + \alpha \left(e^{-\frac{r}{M}} - \frac{2M}{e^2 r} \right)$. The vierbein fields of the hairy extreme spacetime metric, required to find $\gamma^a e^{\mu}_a$, are given by

$$e^t_0 = \frac{1}{\sqrt{f(r)}}, \quad e^r_1 = \sqrt{f(r)}, \tag{43}$$

$$e^\theta_2 = \frac{1}{r}, \quad e^\phi_3 = \frac{1}{r \sin \theta}. \tag{44}$$

Hence, the representation of γ^σ matrices are chosen accordingly:

$$e^t_0 \gamma^0 = \frac{i}{\sqrt{f(r)}} \begin{pmatrix} \mathbb{I}_2 & 0 \\ 0 & -\mathbb{I}_2 \end{pmatrix}, \quad e^r_1 \gamma^1 = \sqrt{f(r)} \begin{pmatrix} 0 & \sigma^3 \\ \sigma^3 & 0 \end{pmatrix}, \tag{45}$$

$$e^\theta_2 \gamma^2 = \frac{1}{r} \begin{pmatrix} 0 & \sigma^1 \\ \sigma^1 & 0 \end{pmatrix}, \quad e^\phi_3 \gamma^3 = \frac{1}{r \sin \theta} \begin{pmatrix} 0 & \sigma^2 \\ \sigma^2 & 0 \end{pmatrix}. \tag{46}$$

Substituting Equations (45) and (46) into Equation (38) and considering the leading order of \hbar , one can find the following system of equations

$$-iA \frac{1}{\sqrt{f}} \partial_t I_\uparrow + (Am - B\sqrt{f} \partial_r I_\uparrow) (\beta\Lambda - 1 + \beta m^2) = 0, \tag{47}$$

$$iB \frac{1}{\sqrt{f}} \partial_t I_\uparrow + (Bm - A\sqrt{f} \partial_r I_\uparrow) (\beta\Lambda - 1 + \beta m^2) = 0, \tag{48}$$

$$A \left[\left(\frac{\partial_\theta I_\uparrow}{r} + i \frac{\partial_\phi I_\uparrow}{r \sin \theta} \right) (\beta\Lambda - 1 + \beta m^2) \right] = 0, \tag{49}$$

$$B \left[\left(\frac{\partial_\theta I_\uparrow}{r} + i \frac{\partial_\phi I_\uparrow}{r \sin \theta} \right) (\beta\Lambda - 1 + \beta m^2) \right] = 0, \tag{50}$$

$$\sqrt{f} (\partial_r I_\uparrow)^2 + \frac{1}{r} (\partial_\theta I_\uparrow)^2 + \frac{1}{r \sin \theta} (\partial_\phi I_\uparrow)^2 = \Lambda. \tag{51}$$

Note that Equations (49) and (50) are the same, regardless of A and B . This means that the inward and outward tunneling angular equations are the same. Consequently, the contribution from $J(\theta, \phi)$ cancels out upon dividing the outcoming probability by the incoming probability [45]. However, they shall be used to simplify the system. The spacetime symmetry motivates the ansatz

$$I_\uparrow = -\omega t + W(r) + J(\theta, \phi). \tag{52}$$

Replacing it in Equation (49) or (50) provides

$$\left(\partial_\theta J(\theta, \phi) + \frac{i}{\sin \theta} \partial_\phi J(\theta, \phi) \right) (\beta\Lambda - 1 + \beta m^2) = 0, \tag{53}$$

which implies $\partial_\theta J(\theta, \phi) + \frac{i}{\sin \theta} \partial_\phi J(\theta, \phi) = 0$, as the second term of Equation (53) does not vanish [43]. Consequently,

$$\left[\frac{1}{r} \partial_\theta J(\theta, \phi) \right]^2 + \left[\frac{1}{r \sin \theta} \partial_\phi J(\theta, \phi) \right]^2 = 0. \tag{54}$$

Using Equations (52) and (54) into (47) and (48) yield the solution to the radial action. Neglecting higher-order terms of β and taking f near the horizon, we can find the particle's tunneling rate, as determined by the imaginary part of the radial action

$$\begin{aligned} \text{Im} W_\pm(r) &= \pm \text{Im} \int dr \frac{1}{f} \sqrt{m^2 f + \omega^2} \left(1 + \beta m^2 + \beta \frac{\omega^2}{f} \right) \\ &= \pm \pi \left(\frac{3 M m^2 \beta \omega e^2}{\sqrt{\alpha^2 - 2 \alpha e^2 + e^4}} + \frac{2 M \omega e^2}{\sqrt{\alpha^2 - 2 \alpha e^2 + e^4}} \right), \end{aligned} \tag{55}$$

$$= \mp \frac{2 \pi M \omega}{1 - \frac{\alpha}{e^2}} \left(1 + \frac{3}{2} m^2 \beta \right), \tag{56}$$

where W_+ (W_-) corresponds to outward (inward) solution. As the overall tunnelling probability is

$$\Gamma = \frac{\Gamma_+}{\Gamma_-} = \frac{e^{-2\text{Im}I_+}}{e^{-2\text{Im}I_-}} = e^{-2\text{Im}(I_+ - I_-)}, \tag{57}$$

in the present case, the tunneling rate of fermions at the event horizon is

$$\Gamma = \frac{e^{-2\text{Im}W_+ - 2J(\theta, \phi)}}{e^{-2\text{Im}W_- - 2J(\theta, \phi)}} = e^{-2\text{Im}(W_+ - W_-)}, \tag{58}$$

$$= \exp \left[\frac{8\pi M\omega}{1 - \frac{\alpha}{e^2}} \left(1 + \frac{3}{2}m^2\beta \right) \right]. \tag{59}$$

This is the Boltzmann factor for an object with the effective temperature

$$T_H = \frac{1}{8\pi M} \frac{1 - \frac{\alpha}{e^2}}{1 + \frac{3}{2}m^2\beta} \simeq T_{\text{Shw}} \left(1 - \frac{\alpha}{e^2} \right) \left(1 - \frac{3}{2}m^2\beta \right). \tag{60}$$

Apart from the hairy parameter α , the quantum effects coming from GUP explicitly reduce the temperature during the evaporation process. This agrees with previous investigations into remnants of black holes [40,43,49]. In this picture, a black hole ceases to radiate when approaching the Planck scale, while its effective temperature reaches a maximum value, leaving a remnant black hole [40]. The combined effects of the deformation parameter α and quantum parameter β strengthen the hypothesis of a vanishing Hawking emission. It is also curious to notice the existence of a fine-tuning between both GUP and deformation parameters, namely, $\beta = -2\alpha/3m^2e^2$, whose net effect is to cancel out both contributions to the Hawking temperature, restoring the standard temperature found for the usual Schwarzschild case.

4. Conclusions

In this paper, some classical and semi-classical effects that occurred near the horizon of a recently discovered class of hairy black holes were investigated. Such black holes were derived by applying the gravitational decoupling technique [18]. In particular, the role of the hairy parameters was analysed on the cross-section expansion along null normals, the surface gravitational constant, Hawking radiation, thermodynamics stability and the generalized Hawking radiation derived from the generalized uncertainty principle. For the latter, we applied the tunnelling method to the generalized Dirac equation. This shows that, apart from the severe attenuation caused by the presence of hair, the quantum parameter β proceeds the suppression. This strengthens the hypothesis of a remnant after a vanishing Hawking emission, as explored in [40,43,49]. Such effects are important theoretical and phenomenological features of black holes, but unfortunately not observationally accessible at the present date. Our results also show that the exotic behavior of hairy black holes occur for the choice of parameters that are close to, but not equal to, the extreme case ($\ell = 2Me^{-2}$), and a horizon radius close to $r_H = 2M$. This could be further explored when searching for effects with observational signature. Another intriguing possibility in our results is that the quantum β and deformation α parameters' combined effects allow for the existence of a fine-tuning, namely, $\beta = -2\alpha/3m^2e^2$, which prevents the Hawking temperature from deviating from $\frac{1}{8\pi M}$, corresponding to the temperature of the Schwarzschild black hole.

Author Contributions: Conceptualization, R.T.C.; Formal analysis, R.T.C., K.d.S.A. and J.M.H.d.S.; Investigation, R.T.C., K.d.S.A. and J.M.H.d.S.; Writing—original draft, R.T.C., K.d.S.A. and J.M.H.d.S. All authors have read and agreed to the published version of the manuscript.

Funding: K.S.A. is grateful to the Coordenação de Aperfeiçoamento de Pessoal de Nível Superior—Brasil (CAPES), Finance Code 001 and grant No 2021/03625-8, São Paulo Research Foundation (FAPESP) for financial support. J.M.H.S. thanks to CNPq (grant No. 303561/2018-1) for financial support.

Data Availability Statement: Not applicable.

Conflicts of Interest: The authors declare no conflict of interest.

References

1. Cardoso, V.; Pani, P. Testing the nature of dark compact objects: A status report. *Living Rev. Rel.* **2019**, *22*, 4. [[CrossRef](#)]
2. Romero, G.E.; Vila, G.S. *Introduction to Black Hole Astrophysics*; Springer: Berlin/Heidelberg, Germany, 2013; Volume 876.
3. Calmet, X. *Quantum Aspects of Black Holes*; Springer: Berlin/Heidelberg, Germany, 2015; Volume 178.
4. Gillessen, S.; Eisenhauer, F.; Trippe, S.; Alexander, T.; Genzel, R.; Martins, F.; Ott, T. Monitoring stellar orbits around the Massive Black Hole in the Galactic Center. *Astrophys. J.* **2009**, *692*, 1075–1109. [[CrossRef](#)]
5. Ghez, A.M.; Salim, S.; Weinberg, N.N.; Lu, J.R.; Do, T.; Dunn, J.K.; Matthews, K.; Morris, M.R.; Yelda, S.; Becklin, E.E. Measuring Distance and Properties of the Milky Way's Central Supermassive Black Hole with Stellar Orbits. *Astrophys. J.* **2008**, *689*, 1044–1062. [[CrossRef](#)]
6. Abbott, B.P.; Abbott, R.; Abbott, T.D.; Abernathy, M.R.; Acernese, F.; Ackley, K.; Adams, C.; Adams, T.; Addesso, P.; Adhikari, R.X.; et al. Observation of Gravitational Waves from a Binary Black Hole Merger. *Phys. Rev. Lett.* **2016**, *116*, 061102. [[CrossRef](#)] [[PubMed](#)]
7. Akiyama, K.; Alberdi, A.; Alef, W.; Asada, K.; Azulay, R.; Baczkó, A.K.; Ball, D.; Baloković, M.; Barrett, J.; Bintley, D.; et al. First M87 Event Horizon Telescope Results. V. Physical Origin of the Asymmetric Ring. *Astrophys. J. Lett.* **2019**, *875*, L1.
8. Frolov, V.P.; Zelnikov, A. *Introduction to Black Hole Physics*; Oxford University Press: Oxford, UK, 2011.
9. Faraoni, V. *Cosmological and Black Hole Apparent Horizons*; Springer: Berlin/Heidelberg, Germany, 2015; Volume 907, ISBN 978-3-319-19239-0/978-3-319-19240-6.
10. Wald, R.M. *General Relativity*; Chicago University Press: Chicago, IL, USA, 1984.
11. Ashtekar, A.; Galloway, G.J. Some uniqueness results for dynamical horizons. *Adv. Theor. Math. Phys.* **2005**, *9*, 1–30. [[CrossRef](#)]
12. Gourgoulhon, E.; Jaramillo, J.L. New theoretical approaches to black holes. *New Astron. Rev.* **2008**, *51*, 791–798. [[CrossRef](#)]
13. Chrusciel, P. *Geometry of Black Holes*; International Series of Monographs on Physics; Oxford University Press: Oxford, UK, 2020; ISBN 978-0-19-885541-5.
14. Babichev, E.; Charmousis, C. Dressing a black hole with a time-dependent Galileon. *JHEP* **2014**, *8*, 106. [[CrossRef](#)]
15. Cavalcanti, R.T.; da Silva, A.G.; da Rocha, R. Strong deflection limit lensing effects in the minimal geometric deformation and Casadio-Fabbri-Mazzacurati solutions. *Class. Quant. Grav.* **2016**, *33*, 215007. [[CrossRef](#)]
16. Ovalle, J. Decoupling gravitational sources in general relativity: From perfect to anisotropic fluids. *Phys. Rev. D* **2017**, *95*, 104019. [[CrossRef](#)]
17. Ovalle, J. Decoupling gravitational sources in general relativity: The extended case. *Phys. Lett. B* **2019**, *788*, 213–218. [[CrossRef](#)]
18. Ovalle, J.; Casadio, R.; Contreras, E.; Sotomayor, A. Hairy black holes by gravitational decoupling. *Phys. Dark Univ.* **2021**, *31*, 100744. [[CrossRef](#)]
19. Da Rocha, R. MGD Dirac Stars. *Symmetry* **2020**, *12*, 508. [[CrossRef](#)]
20. Fernandes-Silva, F.; Malaver, M.; Rincón, A.; Gomez-Leyton, Y. Relativistic anisotropic fluid spheres satisfying a non-linear equation of state. *Eur. Phys. J. C* **2020**, *80*, 371. [[CrossRef](#)]
21. Da Rocha, R. Minimal geometric deformation of Yang-Mills-Dirac stellar configurations. *Phys. Rev. D* **2020**, *102*, 024011. [[CrossRef](#)]
22. Fernandes-Silva, A.; Ferreira-Martins, A.J.; da Rocha, R. Extended quantum portrait of MGD black holes and information entropy. *Phys. Lett.* **2019**, *B791*, 323–330. [[CrossRef](#)]
23. Da Rocha, R. Dark $SU(N)$ glueball stars on fluid branes. *Phys. Rev.* **2017**, *D95*, 124017. [[CrossRef](#)]
24. Da Rocha, R.; Tomaz, A.A. Holographic entanglement entropy under the minimal geometric deformation and extensions. *Eur. Phys. J. C* **2019**, *79*, 1035. [[CrossRef](#)]
25. Ovalle, J.; Contreras, E.; Stuchlik, Z. Kerr-de Sitter black hole revisited. *Phys. Rev. D* **2021**, *103*, 084016. [[CrossRef](#)]
26. Meert, P.; da Rocha, R. Gravitational decoupling, hairy black holes and conformal anomalies. *Eur. Phys. J. C* **2022**, *82*, 175. [[CrossRef](#)]
27. Cavalcanti, R.T.; de Paiva, R.C.; da Rocha, R. Echoes of the gravitational decoupling: Scalar perturbations and quasinormal modes of hairy black holes. *arXiv* **2022**, arXiv:2203.08740.
28. Gross, D.J.; Mende, P.F. String theory beyond the Planck scale. *Nucl. Phys. B* **1988**, *303*, 407–454. [[CrossRef](#)]
29. Amati, D.; Ciafaloni, M.; Veneziano, G. Can spacetime be probed below the string size? *Phys. Lett. B* **1989**, *216*, 41–47. [[CrossRef](#)]
30. Rovelli, C.; Smolin, L. Discreteness of area and volume in quantum gravity. *Nucl. Phys. B* **1995**, *442*, 593–622. Erratum in *Nucl. Phys. B* **1995**, *456*, 753–754. [[CrossRef](#)]
31. Scardigli, F. Generalized uncertainty principle in quantum gravity from micro-black hole gedanken experiment. *Phys. Lett. B* **1999**, *452*, 39–44. [[CrossRef](#)]
32. Hoff da Silva, J.M.; Beghetto, D.; Cavalcanti, R.T.; Da Rocha, R. Exotic fermionic fields and minimal length. *Eur. Phys. J. C* **2020**, *80*, 727. [[CrossRef](#)]
33. Hossenfelder, S. Minimal Length Scale Scenarios for Quantum Gravity. *Living Rev. Rel.* **2013**, *16*, 2. [[CrossRef](#)]
34. Tawfik, A.N.; Diab, A.M. A review of the generalized uncertainty principle. *Rept. Prog. Phys.* **2015**, *78*, 126001. [[CrossRef](#)]

35. Bishop, M.; Contreras, J.; Singleton, D. A Subtle Aspect of Minimal Lengths in the Generalized Uncertainty Principle. *Universe* **2022**, *8*, 192. [[CrossRef](#)]
36. Ashtekar, A.; Krishnan, B. Isolated and Dynamical Horizons and Their Applications. *Living Rev. Rel.* **2004**, *7*, 10. [[CrossRef](#)]
37. Hawking, S.W.; Page, D.N. Thermodynamics of black holes in anti-de Sitter space. *Commun. Math. Phys.* **1983**, *87*, 577. [[CrossRef](#)]
38. Kempf, A.; Mangano, G.; Mann, R.B. Hilbert space representation of the minimal length uncertainty relation. *Phys. Rev. D* **1995**, *52*, 1108–1118. [[CrossRef](#)] [[PubMed](#)]
39. Greiner, W. *Relativistic Quantum Mechanics*; Springer: Berlin/Heidelberg, Germany, 2000; Volume 2.
40. Nozari, K.; Saghafi, S. Natural cutoffs and quantum tunneling from black hole horizon. *JHEP* **2012**, *11*, 5. [[CrossRef](#)]
41. Nozari, K.; Karami, M. Minimal Length and Generalized Dirac Equation. *Mod. Phys. Lett. A* **2005**, *20*, 3095–3104. [[CrossRef](#)]
42. Hossenfelder, S.; Bleicher, M.; Hofmann, S.; Ruppert, J.; Scherer, S.; Stoecker, H. Signatures in the Planck regime. *Phys. Lett. B* **2003**, *575*, 85–99. [[CrossRef](#)]
43. Chen, D.; Wu, H.; Yang, H. Observing remnants by fermions' tunneling. *JCAP* **2014**, *3*, 36. [[CrossRef](#)]
44. Page, D.N. Particle emission rates from a black hole: Massless particles from an uncharged, nonrotating hole. *Phys. Rev. D* **1976**, *13*, 198–206. [[CrossRef](#)]
45. Kerner, R.; Mann, R.B. Fermions tunnelling from black holes. *Class. Quant. Grav.* **2008**, *25*, 095014. [[CrossRef](#)]
46. Barducci, A.; Casalbuoni, R.; Lusanna, L. Supersymmetries and the pseudoclassical relativistic electron. *Nuovo Cim. A* **1976**, *35*, 377. [[CrossRef](#)]
47. Vanzo, L.; Acquaviva, G.; Di Criscienzo, R. Tunnelling methods and Hawking's radiation: achievements and prospects. *Class. Quant. Grav.* **2011**, *28*, 183001. [[CrossRef](#)]
48. Cavalcanti, R.; da Rocha, R. Dark Spinors Hawking Radiation in String Theory Black Holes. *Adv. High Energy Phys.* **2016**, *2016*, 4681902. [[CrossRef](#)]
49. Casadio, R.; Nicolini, P.; da Rocha, R. Generalised uncertainty principle Hawking fermions from minimally geometric deformed black holes. *Class. Quant. Grav.* **2018**, *35*, 185001. [[CrossRef](#)]